PROCEEDINGS, Twelfth Workshop on Geothermal Reservoir Engineering
Stanford University, Stanford, California, January 20-22, 1987
SGP-TR-109

LINEAR WATER INFLUX OF AN INFINITE AQUIFER THROUGH A PARTIALLY COMMUNICATING FAULT

Anil K. Ambastha and Abraham Sageev

Stanford University

Stanford, CA 94305

ABSTRACT

This paper presents a linear flow water influx analysis method where the aquifer is separated from the reservoir by a partially communicating fault. Transient pressure distributions are considered both in the reservoir and in the aquifer. Cases where the leaky fault is located within the aquifer can be analyzed with this model given a superposition of constant rate flow periods at the oil-water interface. Constant production rate is specified at the inner boundary, without inner boundary storage and skin. The partially communicating fault is modeled as a boundary skin of infinitesimal thickness having no storage. The aquifer considered in this paper is infinite in the lateral extent. The problem is posed and solved using the Laplace transformation, yielding Laplace solutions of the exponential form.

The solutions presented in this paper, along with a set of type curves extend the transient linear flow work presented by *Hurst* (1958) and by *Nabor and Barham* (1964). When the inner region, the reservoir, has an infinite permeability and a finite storage, it acts like a tank, where the boundary pressure is equal to average pressure in the inner region. This case is identical to the linear water influx model presented by *Hurst* (1958). When the inner region has no storage associated with it, the constant inner boundary rate is transmitted to the second infinite region, hence yielding the simple linear flow case presented by *Nabor and Barham* (1964).

This paper extends the current solutions by allowing pressure variations in the reservoir or the inner region as well as in the infinite aquifer. Also, the model presented in this paper considers the effects of skin located at the boundary between the two regions of the system that may be caused by a partially communicating fault separating these two regions.

INTRODUCTION

Techniques for reservoir performance calculations for linear and radial water-drive systems have been developed in a series of papers by *van Everdingen and Hurst* (1949), *Hurst* (1958) and *van Everdingen* et al. (1953). In such reservoir performance calculations, one of the following two conditions may be encountered:

1. Given a reservoir pressure history, we determine cumulative water encroachment for the reservoir-aquifer system.
2. Given reservoir rate history, we determine the pressure decline behavior for the reservoir-aquifer system.

Performing these analyses requires the knowledge of transient pressure or influx behavior of the assumed configuration of reservoir-aquifer system. In addition, the key assumption is that the average reservoir pressure is equal to the pressure at the interface between the two differing regions.

The behavior of linear homogeneous aquifers has been examined in the literature. *Hurst* (1958) considered linear water influx into a hydrocarbon reservoir. In his model, the material balance equations for the reservoir are coupled to the transient linear flow diffusivity equation for the aquifer. Hence, pressure transients in the reservoir are not accounted for, and the main parameter controlling the water influx function is the compressibility ratio between the two parts of the system. *Miller* (1962) studied the behavior of closed outer boundary and infinite aquifers. In his analysis, separate curves were needed for each aquifer size. *Nabor* and *Barham* (1964) extended *Miller's* (1962) equations and presented a single working log-log type curve, that is applicable to any aquifer size. They also included the case of constant pressure outer boundary. Non-homogeneous aquifer responses were generated by *Mueller* (1962) using finite-difference techniques. *Mueller* (1962) considered linear variations of thickness, permeability or porosity-compressibility product with distance. Recently, *Ambastha and Ramey* (1987) obtained a suite of analytical response functions for non-homogeneous aquifers. Their results compared well with Mueller's (1962) results. *Bowman and Crawford* (1962) presented a method for calculating transient pressure distribution in linear semi-infinite water-drive reservoirs having different rock and fluid properties in each zone.

A true composite system has two distinct regions, with different properties in each region, as shown in Figure 1. In such a composite system, pressure transients are allowed to develop in both regions. When the inner region has infinite transmissivity and a finite storativity, it acts like a tank, where the boundary pressure is equal to average pressure in the inner region. This case is identical to the linear water influx model presented by *Hurst* (1958). If the inner region has no storativity associated with it, the constant inner boundary rate is transmitted to the second infinite region, hence, yielding the simple linear flow case presented by *Nabor* and *Barham* (1964). Alternatively, a composite system with the same transmissivity and storativity in both regions is identical to the linear semi-infinite homogeneous aquifer model discussed by *Miller* (1962), and *Nabor* and *Barham* (1964). Thus, we can view regions I and II as reservoir and aquifer portions respectively, as an analogy to *Hurst* (1958) model, or consider both regions as an aquifer system extending across a boundary, as an analogy to *Miller* (1962), and *Nabor* and *Barham* (1964) models.

The above discussion implicitly assumes that the boundary separating the two regions of composite system is

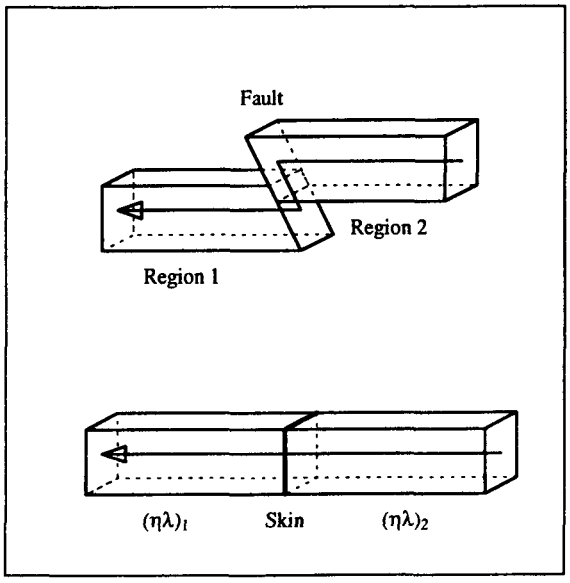

Figure 1: Schematic representation of a composite system.

fully communicating. However, since these boundaries may be created due to geological factors, such as faulting, facies changes or pinchouts, it is possible that these boundaries will resist the flow across them, and be partially communicating. We model this resistance using the "thin skin" concept similar to that proposed by *Hurst* (1953), *van Everdingen* (1953), and *Carslaw* and *Jaeger* (1959). We term it "boundary skin" to distinguish it from "wellbore skin" in the usual sense. In this study we present an analytical solution to the transient flow problem in a linear semi-infinite composite system with property contrasts and boundary skin. Constant rate is specified at the inner boundary. Though the problem is solved with property contrasts in the two regions, we mainly present the results for homogeneous systems with boundary skin. The relationship of the general model to *Hurst* (1958), and *Nabor* and *Barham* (1964) models is presented. Late and early time behavior for special cases are developed. A type curve is presented for homogeneous systems with boundary skin. Finally, a modification of Example No. 2 of *Nabor* and *Barham* (1964) has been solved under different model conditions to demonstrate the effects of boundary skin.

MATHEMATICAL CONSIDERATIONS

The geometrical configuration considered is presented in Figure 2. The dimensionless diffusivity equations describing the pressure response of a semi-infinite composite horizontal linear system are:

$$\frac{\partial^2 p_{D1}}{\partial x_D^2} = \frac{\partial p_{D1}}{\partial t_D} \qquad \text{for} \quad 0 \le x_D \le A \tag{1}$$

$$\frac{\partial^2 p_{D2}}{\partial x_D^2} = \frac{1}{\eta}\frac{\partial p_{D2}}{\partial t_D} \qquad \text{for} \quad A \le x_D \le \infty \tag{2}$$

where the dimensionless variables are defined as:

$$p_{D1} = \frac{k_1 bh\,[p_i - p_1(x,t)]}{q\mu_1\ 1} \tag{3}$$

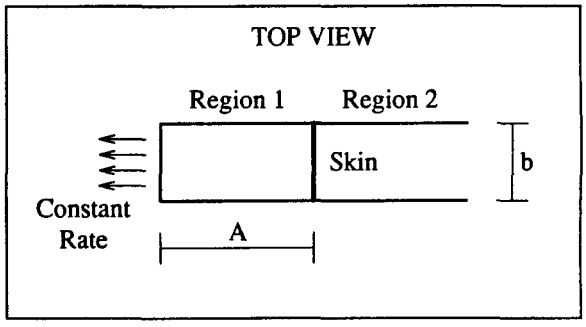

Figure 2: Simplified linear composite system.

$$p_{D2} = \frac{k_1 bh\,[p_i - p_2(x,t)]}{q\mu_1\ 1} \tag{4}$$

$$x_D = \frac{x}{1} \tag{5}$$

$$t_D = \frac{k_1 t}{(\phi\mu c_t)_1\ 1^2} \tag{6}$$

$$\eta = \frac{\eta_2}{\eta_1} = \frac{\left[\dfrac{k}{\phi\mu c_t}\right]_2}{\left[\dfrac{k}{\phi\mu c_t}\right]_1} \tag{7}$$

The characteristic length of unity is used in the definitions of dimensionless distance, pressure and time. The associated initial and outer boundary conditions are:

$$p_{D1}(x_D,0) = 0 \tag{8}$$

$$p_{D2}(x_D,0) = 0 \tag{9}$$

$$p_{D2}(\infty,t_D) = 0 \tag{10}$$

The inner boundary condition is:

$$\left.\frac{\partial p_{D1}}{\partial x_D}\right]_{x_D=0} = -1 \tag{11}$$

The conditions at the skin boundary are:

$$\frac{\partial p_{D1}}{\partial x_D} = \frac{-1}{S}(p_{D1} - p_{D2}) \qquad at\ \ x_D = A \tag{12}$$

$$\frac{\partial p_{D1}}{\partial x_D} = M\frac{\partial p_{D2}}{\partial x_D} \qquad at\ \ x_D = A \tag{13}$$

where S, the boundary skin, is defined by:

$$S = \frac{k_1 bh[p_i - p_1(a,t)]}{q^*\mu_1\ 1} \tag{14}$$

In Equation (14), q^* is the flow rate at the boundary that changes with time. A and M are the dimensionless boundary distance and mobility ratio respectively and are defined by:

$$A = \frac{a}{1} \tag{15}$$

$$M = \frac{\lambda_2}{\lambda_1} = \frac{k_2\mu_1}{k_1\mu_2} \tag{16}$$

The other terms are defined in the nomenclature. Taking the Laplace transformation of Equations (1), (2), and (10) through (13) with respect to the dimensionless time, t_D, using initial conditions of Equations (8) and (9) yields:

$$\frac{d^2\bar{p}_{D1}}{dx_D^2} - s\bar{p}_{D1} = 0 \tag{17}$$

$$\frac{d^2\bar{p}_{D2}}{dx_D^2} - \frac{1}{\eta}\, s\bar{p}_{D2} = 0 \tag{18}$$

$$\bar{p}_{D2}(\infty,s) = 0 \tag{19}$$

$$\left.\frac{d\bar{p}_{D1}}{dx_D}\right]_{x_D=0} = -\frac{1}{s} \tag{20}$$

$$\frac{d\bar{p}_{D1}}{dx_D} = \frac{-1}{S}\,(\bar{p}_{D1}-\bar{p}_{D2}) \qquad at\ \ x_D = A \tag{21}$$

$$\frac{d\bar{p}_{D1}}{dx_D} = M\,\frac{d\bar{p}_{D2}}{dx_D} \qquad at\ \ x_D = A \tag{22}$$

The solutions to the ordinary differential Equations (17) and (18), and the associated boundary conditions, Equations (19) through (22) are:

$$\bar{p}_{D1}(x_D,s) = C_1\, e^{\sqrt{s}\,x_D} + C_2\, e^{-\sqrt{s}\,x_D} \tag{23}$$

$$\bar{p}_{D2}(x_D,s) = C_3\, e^{\sqrt{s/\eta}\,x_D} + C_4\, e^{-\sqrt{s/\eta}\,x_D} \tag{24}$$

The Laplace dimensionless pressure drop at the inner boundary is derived by letting $x_D = 0$:

$$\bar{p}_{wD} = C_1 + C_2 \tag{25}$$

C_1 through C_4 are given by the following expressions:

$$C_1 = \frac{D\left[-1 - \dfrac{M}{\sqrt{\eta}}\,(S\sqrt{s}-1)\right]}{\dfrac{Ms\sqrt{s}}{\sqrt{\eta}}\left[(S\sqrt{s}(D-E) - (D+E)\right] + s\sqrt{s}\,(D-E)} \tag{26}$$

$$C_2 = C_1 + \frac{1}{s\sqrt{s}} \tag{27}$$

$$C_3 = 0 \tag{28}$$

$$C_4 = \frac{(D\,C_2 - E\,C_1)}{\dfrac{M}{\sqrt{\eta}}\; e^{-A\sqrt{s/\eta}}} \tag{29}$$

where D and E are given by:

$$D = e^{-A\sqrt{s}} \tag{30}$$

$$E = e^{A\sqrt{s}} \tag{31}$$

Using Equation (27) in Equation (25) yields:

$$\bar{p}_{wD} = 2C_1 + \frac{1}{s\sqrt{s}} \tag{32}$$

Solutions for some special cases appear next. From Equations (23) and (26), $M/\sqrt{\eta}$ is recognized as a correlating parameter for the dimensionless pressure drop in region I. However, $M/\sqrt{\eta}$ is not a correlating parameter for the dimensionless pressure drop in region II because of the appearance of $\sqrt{s/\eta}$ in the exponential argument in Equation (24).

EARLY AND LATE TIME APPROXIMATIONS

Examination of Equation (26) shows that $C_1 \to 0$ as $s \to \infty$ for arbitrary M, η, S and A. Thus, at early time, $\bar{p}_{wD}$ is:

$$\bar{p}_{wD} = \frac{1}{s\sqrt{s}} \tag{33}$$

that inverts to:

$$p_{wD} = 2\sqrt{\frac{t_D}{\pi}} \tag{34}$$

Equation (34) is the infinite acting homogeneous linear flow solution that was presented by *Nabor* and *Barham* (1964).

At late time, $t \to \infty$ and $s \to 0$. For any set of M, η, S and A, the expression for $2C_1$ at late times is:

$$2C_1 = \frac{1}{\dfrac{M}{\sqrt{\eta}}\, s\,\sqrt{s}} + \frac{S}{s} - \frac{1}{s\sqrt{s}} \tag{35}$$

since $D \to 1$ and $E \to 1$ as $s \to 0$. From Equations (32) and (35), the dimensionless Laplace pressure solution simplifies to:

$$\bar{p}_{wD} = \frac{1}{\dfrac{M}{\sqrt{\eta}}}\,\frac{1}{s\sqrt{s}} + \frac{S}{s} \tag{36}$$

that inverts to:

$$p_{wD} = \frac{2}{\dfrac{M}{\sqrt{\eta}}}\sqrt{\frac{t_D}{\pi}} + S \tag{37}$$

For a homogeneous aquifer ($M = 1$ and $\eta = 1$), Equation (37) reduces to:

$$p_{wD} = 2\sqrt{\frac{t_D}{\pi}} + S \tag{38}$$

RELATIONSHIP WITH *NABOR AND BARHAM* MODEL

We saw that the early time behavior of a composite system with property contrast and boundary skin is given by the *Nabor* and *Barham* (1964) model. Also, Equation (37) shows that in the absence of boundary skin, proper combinations of M and η such that $M/\sqrt{\eta} = 1$ will result in a homogeneous semi-infinite linear aquifer solution as presented by *Nabor* and *Barham* (1964). Actually, in such a case when $M/\sqrt{\eta} = 1$ and $S = 0$, even the intermediate time behavior is the same as *Nabor* and *Barham* (1964) model as shown in Figure 3.

Also, if the inner region has a low storativity associated with it, a specified real time corresponds to a large t_D, and the system behavior will be given by Equation (37). Hence, we would have a half slope on a log-log graph similar to that obtained for *Nabor* and *Barham* (1964) linear semi-infinite aquifer model.

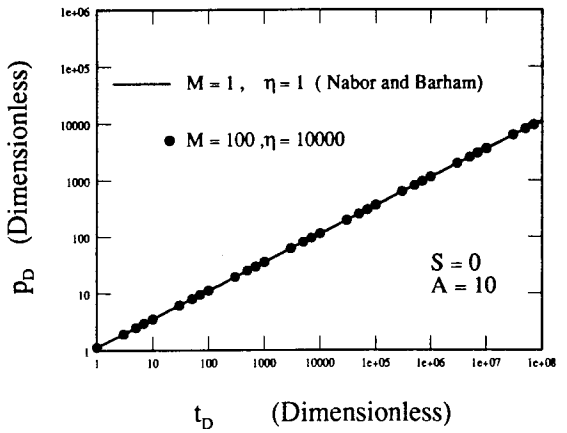

Figure 3: Comparison with the *Nabor* and *Barham* (1964) model.

RELATIONSHIP WITH *HURST* MODEL

Equation (17) of *Hurst's* (1958) paper representing linear water influx model is:

$$\Delta p = \frac{\phi \mu_w c_w q_o}{k N c_o \lambda^2} f(\lambda \sqrt{t_D}) \tag{39}$$

where

$$t_D = \frac{kt}{\phi \mu_w c_w 1^2} \tag{40}$$

$$\lambda = \frac{bh\phi c_w}{NB_{oi}c_o} \tag{41}$$

$$f(\lambda \sqrt{t_D}) = e^{\lambda^2 t_D} erfc(\lambda\sqrt{t_D}) - 1 + 2\lambda\sqrt{t_D/\pi} \tag{42}$$

and other terms are defined in *Hurst's* (1958) paper. In our notation, the *Hurst* (1958) model is represented as:

$$\lambda p_D = f(\lambda \sqrt{t_D}) \tag{43}$$

where

$$\lambda = \frac{(\phi c_t)_2}{A (\phi c_t)_1} \tag{44}$$

$$p_D = \frac{k_2 bh\Delta p}{\mu_2 q} \tag{45}$$

$$t_D = \frac{k_2 t}{(\phi \mu c_t)_2 1^2} \tag{46}$$

The subscripts 1 and 2 refer to region I (oil zone) and region II (aquifer zone) respectively. Equation (43) shows that *Hurst* (1958) model can be represented by just one curve if λp_D is graphed against $\lambda\sqrt{t_D}$. The solid line in Figure 4 is the *Hurst* (1958) model. Circles represent the computation using the general solution developed in this study with M = 0.001, A = 10, S = 0 and η = 1. The agreement between the two models shows that the behavior of the system with a high transmissivity and a finite storativity in the inner region representing the reservoir is identical to the linear water influx model presented by *Hurst* (1958).

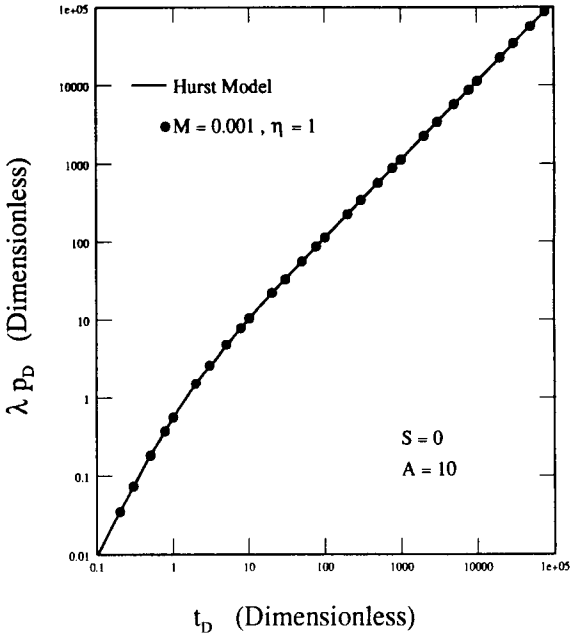

Figure 4: Comparison with the *Hurst* (1958) model.

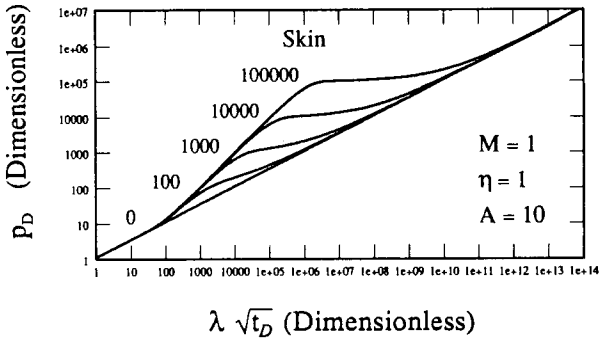

Figure 5: Effects of boundary skin on dimensionless pressure responses.

TYPE CURVE DEVELOPMENT

The Laplace solution of Equation (32) was inverted numerically using an algorithm developed by *Stehfest* (1970). Figure 5 examines the effects of boundary skin with a fixed distance to the boundary. All the curves are identical at early time as predicted by Equation (34), representing the infinite acting linear flow period controlled by the properties of the inner region. The infinite acting linear flow period is characterized by a one half slope on the log-log graph. All the curves depart from the infinite acting behavior at the same time, doubling the slope to unity, representing pseudo steady state (PSS) depletion of the inner region. Then, depending on the value of boundary skin, the pressure response tends to stabilize, joining at late time the infinite acting linear pressure response. The higher the value of boundary skin, the longer is the PSS flow period. Also, the late time curves are separated by the value of boundary skin, as predicted by Equation (38), but due to the log-log presentation, the constant difference

Table 1: Late Time Dimensionless Pressure Drop at the Inner Boundary for Unit Mobility and Diffusivity Ratio

Skin	0	10^3	10^4	10^5	10^6
$t_D\ 10^{-12}$	$p_D\ 10^{-6}$	$p_D\ 10^{-6}$	$p_D\ 10^{-6}$	$p_D\ 10^{-6}$	$p_D\ 10^{-6}$
1	1.128	1.129	1.138	1.228	2.128
5	2.523	2.524	2.533	2.623	3.523
10	3.568	3.569	3.578	3.668	4.568
50	7.979	7.980	7.989	8.079	8.979
100	11.28	11.28	11.29	11.38	12.28
500	25.23	25.23	25.24	25.33	26.3

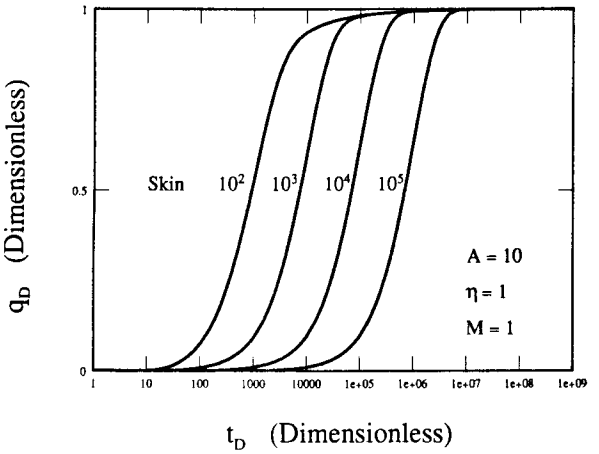

Figure 6: Dimensionless influx rate across the fault for different values of skin.

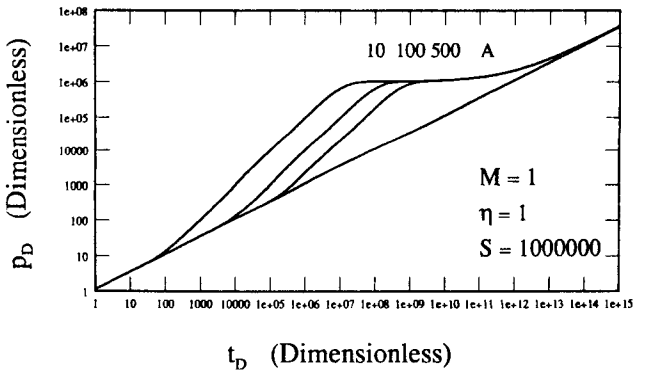

Figure 7: Effects of boundary distance on dimensionless pressure responses.

is not visible. This separation at late time is presented in Table 1.

Figure 6 presents the effect of boundary skin on the dimensionless influx rate for a fixed boundary distance. The dimensionless influx rate is zero at early time, characterizing the infinite acting linear flow period controlled by the properties of the inner region. The duration of the transition from an influx rate of zero to one depends on the value of the boundary skin. As the boundary skin increases, the significant flow across the fault is delayed. Thus, the pseudo steady state depletion lasts longer for larger value of boundary skin, as seen in Figure 5. Once an appreciable influx starts occurring across the fault, the pressure response tends to stabilize (See Figure 5). Finally, the dimensionless influx rate becomes one that corresponds to the late time infinite acting linear flow period. Hence, Figure 6 provides a physical explanation for the pressure behavior observed in Figure 5.

Table 2: Dimensionless Departure Time Data for Linear Semi-infinite Homogeneous Systems with Boundary Skin

A	$t_{D,d}$	$\sqrt{t_{D,d}}$	C
10	40	6.32	1.581
50	1,000	31.62	1.581
100	4,000	63.24	1.581
500	100,000	316.2	1.581

Note: $C = \dfrac{A}{\sqrt{t_{D,d}}}$

Figure 7 presents the effects of boundary distance with a fixed value of boundary skin. The departure of the pressure response from the infinite acting linear flow period is controlled by boundary distance. As A increases, the departure time is delayed. Table 2 lists the dimensionless departure times for different values of A, and a linear correlation between the square root of dimensionless departure time and dimensionless boundary distance is presented in Figure 8. This correlation is independent of boundary skin, and is described by:

$$A = 1.581\ \sqrt{t_{D,d}} \qquad (47)$$

The effects of the boundary distance and skin on the pressure response are presented in Figure 9. Here, the lowermost thick curve represents infinite linear flow behavior. The onset of the unit slope representing PSS flow (or equivalently, the departure of the pressure response from the infinite acting flow period) is controlled by the value of the distance to the boundary. The stabilized portions of the curves are controlled by the value of the boundary skin. The curves in Figure 9 can be correlated by shifting them horizontally and vertically in some manner. Figure 10 shows an example of the curve for A = 100 and S = 1000 shifted and matched to the curve for A = 10 and S = 100. Numerically, the two curves match within less than 0.1%. Thus, the behavior of homogeneous semi-infinite aquifers with boundary skin is summarized as a type curve presented in Figure 11 that applies for all values of A. We arbitrarily chose to correlate all the curves with the curves for A = 10. Any other choice of A would also have sufficed.

Matching reservoir data to the type curve presented in Figure 11 offers a method for detecting the boundary and also determining if there is a skin associated with this boundary. However, the determination of the values of A and S is not unique. If we have the distance to the boundary, we can estimate the magnitude of the skin. Also, this type curve may help examining the possible ranges of A and S for a given set of data, hence helping in setting some realistic limits on the distribution of reservoir heterogeneities.

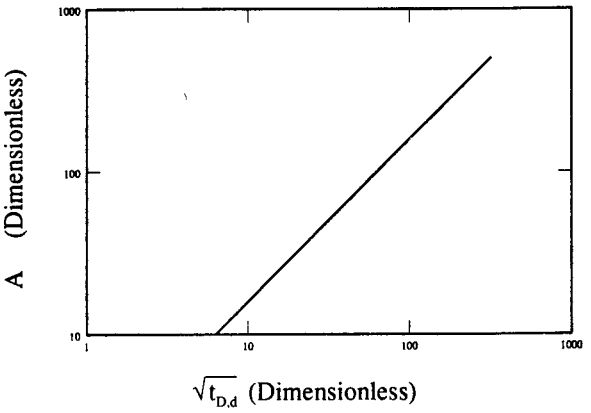

Figure 8: Correlation between dimensionless boundary distance and dimensionless departure time.

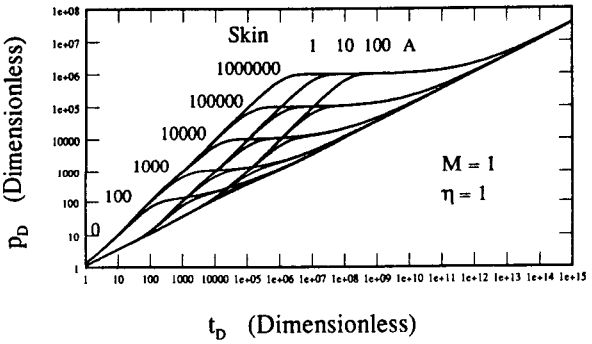

Figure 9: Combined effects of boundary distance and skin on pressure responses.

EXAMPLE CALCULATION

We solve a modification of Example No. 2 of *Nabor* and *Barham* (1964) for different cases to demonstrate how to use the type curve of Figure 10. The example involves estimation of the pressure drop at the aquifer-reservoir boundary for a constant influx rate of 53.1 bbl/Day over a 91 day time period. Aquifer properties are given in Table 3. We assume the boundary distance to be 1000 ft (ie, A = 1000). To apply *Nabor* and *Barham* (1964) model, we assume the aquifer length, L, to be 1000 ft. Thus, for the *Nabor* and *Barham* (1964) model,

$$t_{D,N+B} = \frac{kt}{\phi\mu c_t L^2}$$

$$= \frac{(1.8985)\ (91)}{(0.25)\ (1)\ (6.2 \times 10^{-6})\ (1000^2)} = 111.5 \quad (48)$$

However, for our model,

$$t_D = \frac{kt}{\phi\mu c_t} = 111.5 \times 10^6 \quad (49)$$

and therefore

$$t_D(10/A)^2 = 1.1 \times 10^4 \quad (50)$$

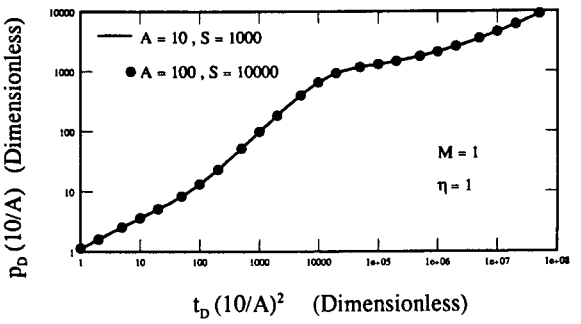

Figure 10: Establishing S/A as a correlating parameter for pressure responses.

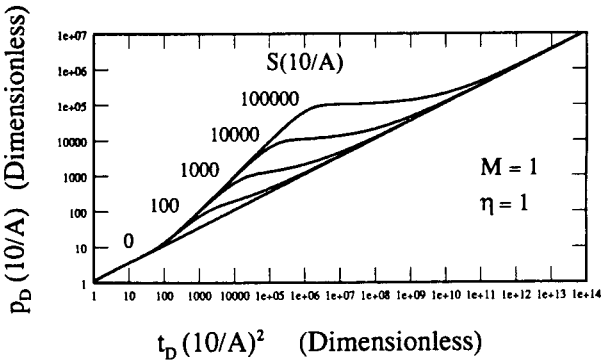

Figure 11: Type curve for linear infinite homogeneous systems with boundary skin.

Table 3: Aquifer Properties (after *Nabor* and *Barham*, 1964)

Property	Value
b	2000 ft
h	41 ft
k	300 md
ϕ	0.25
μ_w	1 cp
c_t	6.2×10^{-6} psi^{-1}

Calculations required to get p_D values at the above t_D for different boundary skin values are shown in Table 4. The values of p_D x 10/A are read from the type curve of Figure 10. An illustration for getting the p_D x 10/A values for the example calculation is shown in Figure 12.

Table 5 shows the results of pressure drop calculations for different cases. Cases 1 and 2 use the *Nabor* and *Barham* (1964) model and pressure drop is calculated by:

$$\Delta p_{N+B} = \frac{q\mu L}{kbh}\, p_D\,(t_D)$$

$$= \frac{(298.1)\ (1)\ (1000)}{(1.8985)\ (2000)\ (41)} p_D\,(t_D)$$

$$= 1.915\, p_D\,(t_D) \quad (51)$$

Table 4: p_D from Type Curve for $t_D\,(10/A)^2 = 1.1x10^4$

S	10 S/A	p_D x (10/A)	p_D
0	0	119.1	1.19 x 10^4
10^4	10^2	207.7	2.08 x 10^4
10^5	10^3	699.7	7.00 x 10^4
10^6	10^4	1059.1	10.59 x 10^4

Table 5: Pressure Drop Estimations

No.	Case	Model	Δp calc. (psi)
1	Semi-infinite	Nabor and	23
2	Closed, 1000 ft long	Barham	214
3	$S = 0$		23
4	$S = 10^4$	New	40
5	$S = 10^5$	Model	134
6	$S = 10^6$	(Semi-infinite)	203

Table 6: Pressure Drop Estimations at Different Locations

Case	Skin	Calculated Pressure Drop, psi			Average Pressure Drop, psi
		x_D=0	x_D=500	x_D=1000	
3	0	23	22	21	22
4	10^4	40	39	38	39
5	10^5	134	133	132	133
6	10^6	203	202	202	202.3

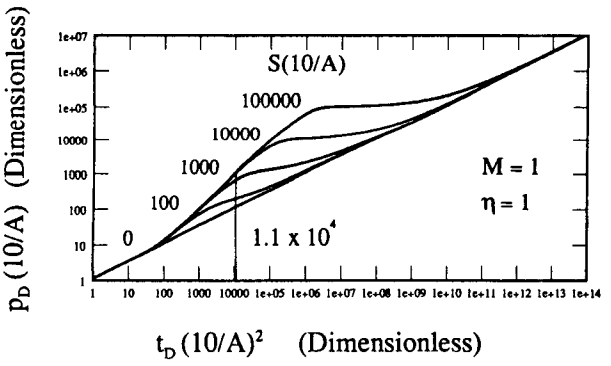

Figure 12: p_D×10/A values from the type curve for t_D×$(10/A)^2$=1.1×10^4.

Cases 3, 4, 5 and 6 use our model and the pressure drop is calculated by:

$$\Delta p = \frac{q\mu}{kbh}\, p_D\,(t_D)$$

$$= 1.915 \times 10^{-3}\, p_D\,(t_D) \qquad (52)$$

Equations (51) and (52) are different because of our definition of p_D. There are two points to be made regarding the pressure drop results in Table 5. The first point is that we need a large boundary skin to create appreciable effect on the influx calculations. Also, the farther the skin boundary, larger the skin needed to create an influx effect. The second point is that ignoring the effect of partially communicating boundaries may result in an incorrect assumption of a closed aquifer that could lead to erroneous results in reserve estimations and history matching.

The calculated pressure drop for our model in Table 5 refers to the production boundary (x_D = 0). However, *Nabor* and *Barham* (1964) model gives the average pressure drop in the inner region. Since our model allows pressure transients to develop in the inner region, pressure drop will be lower as the pressure point moves toward the fault. Figure 13 shows the pressure responses for different locations with a fixed boundary distance and skin. The effect of the location of the pressure point on the pressure response is significant at early time. We re-calculated the pressure drops with our model using different pressure point locations for the example calculation, presented in Table 6. The average pressure drop is calculated as the the average of calculated pressure drops for the three pressure locations The average pressure drop in any case is close to the calculated pressure drop at the production boundary (x_D = 0). Also, since pressure locations only affect the pressure response at early time as in Figure 13, it should be sufficient to calculate pressure drop at the production boundary using our model for most cases. However, we found that x_D x (10/A) and S x (10/A) are the correlating parameters for the pressure responses in the inner region. Figure 14 shows an example of this correlation with x_D x (10/A) = 5 and S x (10/A) = 10^4. Thus, if calculating average pressure drop were necessary, a type curve for the pressure responses in the inner region could be developed using x_D x (10/A) and S x (10/A) as the correlating parameters.

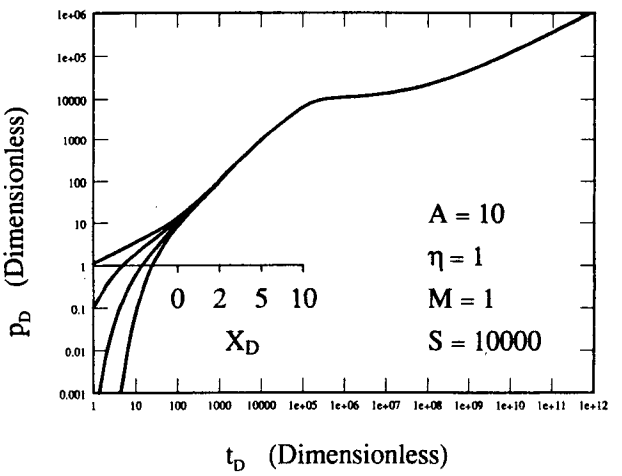

Figure 13: Pressure responses for different locations with a fixed boundary distance and skin.

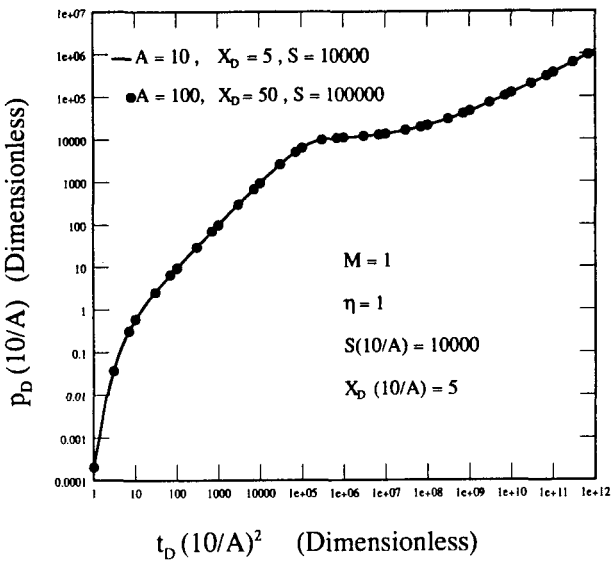

Figure 14: Establishing correlating parameters for pressure responses in the inner region.

CONCLUSIONS

1. The transient pressure behavior of a semi-infinite composite linear system with property contrast and boundary skin has been analytically solved. This paper extends the applicability of the presently known linear influx models. Only constant rate at the inner boundary has been considered.
2. *Hurst* (1958), and *Nabor* and *Barham* (1964) linear influx models are special cases of the new general model described in this paper.
3. The departure of the pressure response at the production boundary from the infinite-acting linear response is only controlled by the distance to the boundary. A linear correlation between the dimensionless boundary distance and the square root of dimensionless departure time is presented.
4. The transition between early and late time infinite acting behavior is explained in terms of the dimensionless influx rate behavior across the fault. The dimensionless influx rate is zero at early time and approaches unity at late time.
5. The pseudo steady state depletion lasts longer for larger value of boundary skin. When appreciable influx starts occurring across the fault, the pressure response tends to stabilize before reaching late time infinite acting linear flow behavior.
6. Boundary skin and the distance to the boundary determine the pressure response for linear homogeneous systems. A type curve is presented in Figure 10 in terms of the correlating parameter 10 *S/A*. Though the results are not presented for composite systems with property contrasts, $M/\sqrt{\eta}$ is the other correlating parameter for pressure responses in region I, as suggested by Equations (23) and (26).
7. A large skin is needed to create an appreciable effect on the influx calculations. However, ignoring the effect of partial communication at the boundary may result in the selection of an improper aquifer model leading to possible errors in reserve estimations and history matching.
8. Different pressure locations in the inner region significantly affect the pressure responses at early time. For most cases, calculating pressure drop at the production boundary should be sufficient.
9. The pressure responses in the inner region can be correlated in terms of the parameters x_D x (10/*A*) and *S* x (10/*A*).

ACKNOWLEDGEMENTS

Financial support was provided by the Stanford Geothermal Program, DOE Contract No. DE-AT02-80SF11459, and by Stanford University.

NOMENCLATURE

A	Dimensionless boundary distance
a	Boundary distance
b	System width
C_1–C_4	Constants in the solutions
c_t	Total system compressibility
D,E	Parameters given by Equations (30) and (31)
h	Thickness
k	Permeability
M	Mobility Ratio
p	Pressure
p_D	Dimensionless pressure
$\bar{p}_D$	Dimensionless pressure drop in Laplace space
p_i	Initial pressure
p_{wD}	Dimensionless pressure drop
q	Influx rate
S	Boundary skin
s	Laplace variable
t	Time
t_D	Dimensionless time
$t_{D,d}$	Dimensionless departure time
x	Distance
x_D	Dimensionless distance

Greek symbols

∂	Partial derivative
η	Diffusivity ratio
λ	Mobility (Also Hurst model parameter as given by Equation (41) or (44))
ϕ	Porosity
μ	Viscosity

Subscripts

1	Zone 1
2	Zone 2
D	Dimensionless
i	Initial
t	Total

REFERENCES

Ambastha, A.K. and Ramey, H.J.,Jr.: "An Analytical Study of Transient Flow in Linear Nonhomogeneous Aquifers," *SUPRI* Tech. Report (to be published).

Bowman, C.H., and Crawford, P.B.: "A Practical Method for Calculating the Transient Pressure Distribution in Linear Semi-infinite Water Driven Reservoirs Having Different Fluid and Rock Properties in Each Zone," SPE Paper 272 (1962).

Carslaw, H.S. and Jaeger, J.S.: *Conduction of Heat in Solids*, second edition, Clarendon Press, Oxford (1959) 18-23.

Hurst, W.: "Establishment of the Skin Effect and Its Impediment to Fluid Flow Into a Well Bore," *The Petroleum Engineer* (Oct. 1953) B6-B16.

Hurst, W.: "The Simplification of the Material Balance Formulas by the Laplace Transformation," *Trans.* AIME (1958) 213, 292.

Miller, F.G.: "Theory of Unsteady-State Influx of Water in Linear Reservoirs," *Journal Institute of Petroleum* (Nov. 1962) 48, 365.

Mueller, T.D.: "Transient Response of Nonhomogeneous Aquifers," *Soc. Pet. Eng. J.* (March 1962) 33-43.

Nabor, G.W., and Barham, R.H.: "Linear Aquifer Behavior," *J. Pet. Tech.* (May 1964) 561-563.

Stehfest, H.: "Algorithm 368, Numerical Inversion of Laplace Transforms," D-5, *Comm. of ACM* ,13, No.1 (Jan. 1970), 49.

Van Everdingen, A.F.: "The Skin Effect and Its Influence on the Productive Capacity of a Well," *Trans.*, AIME (1953) Vol. 198, 171-176.

Van Everdingen, A.F., and Hurst, W.: "The Application of the Laplace Transformation to Flow Problems in Reservoirs," *Trans.*, AIME (1949) Vol. 186, 305.

Van Everdingen, A.F., Timmerman, E.H., and McMahon, J.J.: "Application of the Material Balance Equation to a Partial Water-Drive Reservoir," *Trans.*, AIME (1953) Vol. 198, 51.